

# THE ENVIRONMENTAL DEPENDENCE OF THE INFRARED LUMINOSITY AND STELLAR MASS FUNCTIONS<sup>1</sup>

MICHAEL L. BALOGH<sup>2</sup>

Department of Physics, University of Durham  
 South Road, Durham, UK DH1 3LE

DANIEL CHRISTLEIN, ANN I. ZABLUDOFF & DENNIS ZARITSKY

Steward Observatory, University of Arizona  
 Tucson, AZ, 85721 USA

*Draft version February 1, 2008*

## ABSTRACT

We investigate the dependence of the galaxy infrared luminosity function (LF) and the associated stellar mass function (SMF) on environment and spectral type using photometry from the Two Micron All Sky Survey and redshifts from the Las Campanas Redshift Survey for galaxies brighter than  $M_J < -19 + 5\log h$ . In the field environment, galaxies with emission lines have LFs with much steeper faint end slopes ( $\alpha_J = -1.39$ ) than galaxies without emission lines ( $\alpha_J = -0.59$ ). In the cluster environment, however, even the non-emission line galaxies have a steep faint-end LF ( $\alpha_J = -1.22$ ). There is also a significant (95%) difference between the overall cluster and field LFs,  $\Delta\alpha_J = -0.34$ ,  $\Delta M_J^* = -0.54$ . All of these variations are more pronounced in the SMFs, which we compute by relating the strength of the 4000Å break in the optical spectra to a stellar mass-to-light ratio.

*Subject headings:* galaxies:clusters:general—galaxies:luminosity function—galaxies:mass function—galaxies:evolution—infrared:galaxies

## 1. INTRODUCTION

The shape of the stellar mass function (SMF) is a fundamental property of the galaxy population because it constrains the baryon content of galaxies, the fraction of all baryons in stars, and the chemical evolution of galaxies. Until recently, however, observational work has been unable to provide a reliable, direct estimate of the SMF. This failure arises primarily because the conversion of the luminosity function (LF) into the SMF requires the poorly-constrained optical mass-to-light (M/L) ratio, which in turn depends sensitively on both the stellar populations and the spatial distribution of dust and stars, neither of which is known for a substantial sample of galaxies. Complex models of dust and star formation are therefore required to compare the observations with theoretical predictions (Cole et al. 2000a; Granato et al. 2000).

It is now possible to mitigate these difficulties by combining spectroscopic catalogs with large infrared (IR) surveys. The sensitivity of M/L to stellar populations and extinction, which has plagued the transformation of the optical LF to a SMF, is lessened at IR wavelengths. M/L varies by only a factor of  $\sim$  two over a large range of star formation histories (e.g., Gavazzi, Pierini &

Boselli 1996; Bell & de Jong 2001; Cole et al. 2000a) and is nearly insensitive to the presence of dust at the levels expected in most galaxies (the typical internal extinction at  $K_s$  is  $\sim 0.05$  mag; Silva et al. 1998).

Three recent developments motivate us to attempt the measurement of the SMF's environmental dependence. First, large IR surveys are an entirely new resource, due to the advent of large format detectors, dedicated survey telescopes, and significant human and material resources. Second, the availability and uniform analysis of large optical and IR surveys has led to a consensus on the shape of the *global* galaxy LF at both optical and IR wavelengths. Although controversy persisted for many years regarding differences between the optical LFs obtained by different investigators (e.g., Loveday et al. 1992; Efstathiou et al. 1988; Marzke et al. 1994b; Lin et al. 1996; Zucca et al. 1997; Ratcliffe et al. 1998), these differences have now largely been resolved (Blanton et al. 2000). At IR wavelengths, agreement among different samples has been extraordinarily good (Mobasher et al. 1993; Glazebrook et al. 1995; Gardner et al. 1997; Szokoly et al. 1998; Loveday 2000; Kochanek et al. 2000b; Cole et al. 2000b). This long-awaited concordance

<sup>1</sup>This publication makes use of data products from the Two Micron All Sky Survey (2MASS), which is a joint project of the University of Massachusetts and the Infrared Processing and Analysis Center/California Institute of Technology, funded by the National Aeronautics and Space Administration and the National Science Foundation.

<sup>2</sup>email:M.L.Balogh@durham.ac.uk

makes it possible to confidently proceed and investigate variations in the LF for different galaxy types, different environments, and different redshifts. Third, the availability of large, cosmological simulations allow the dependence of the SMF on environment to be modeled with some reliability. However, the translation from the dark matter halo mass function to the SMF still depends on such complicated and ill-understood factors as the bias function (White et al. 1987; Narayanan et al. 2000), the gas cooling rate (Rees and Ostriker 1977), and reheating due to feedback from star formation (e.g., Larson 1974; Cole 1991; Balogh et al. 2001).

A dependence of the SMF on galaxy type would not be surprising, due to the distinctly different star formation histories of late- and early-type galaxies. In addition, we can expect an environmental dependence of the SMF because (1) the merging history (e.g., Lacey and Cole 1993) and bias level (Bardeen et al. 1986; Narayanan et al. 2000) of halos in clusters are different from those of isolated halos, (2) there are physical processes, such as galaxy harassment (Moore et al. 1999), that may operate in dense cluster environments and alter the halo mass function, and (3) the stellar populations of cluster galaxies are different from those of field galaxies, perhaps indicative of different star formation histories (e.g., Dressler et al. 1985; Balogh et al. 1997; Balogh et al. 1998; Poggianti et al. 1999; Moss and Whittle 2000).

Such expectations have already received some support from observations. It is well known that the optical LF depends on galaxy morphology (e.g., Loveday et al. 1992; Binggeli et al. 1988; Marzke et al. 1994a; Marzke et al. 1998), primarily in the sense that it steepens toward later galaxy types. Analogous trends are also seen if the population is divided by emission line strength (Ellis et al. 1996; Lin et al. 1996; Loveday et al. 1999; Christlein 2000), color (Marzke and da Costa 1997; Lin et al. 1996; Treyer et al. 1998), or principal spectral components (Bromley et al. 1998; Folkes et al. 1999). In addition to the dependence on type, optical observations also indicate that the dwarf-to-giant ratio steadily increases with increasing environmental density (Sandage et al. 1985; de Propris et al. 1995; Ferguson and Sandage 1991; Bromley et al. 1998; Zabludoff and Mulchaey 2000; Christlein 2000).

The trends seen in the optical LFs must be explored in the IR to determine whether they reflect underlying variations in the SMF or in M/L. In

one recent example of such work, Kochanek et al. (2000b) find that the  $K_s$ -band LF of galaxies has the same dependence on morphology as seen at optical wavelengths. This finding is strong evidence that the galactic SMF is not universal, and that early-type galaxies cannot simply be an unbiased subsample of late-type galaxies in which star formation has ceased. Our primary purpose is to further explore in the IR the trends found in the optical. The compilation of the data we use is described in §2. In §3, we calculate the  $J$  and  $K_s$  band galaxy luminosity functions as a function of environment and spectral type. We find that the trends in optical data are also present in the IR data, and more significantly in the stellar mass function. The implications are explored in §4, and we summarize our conclusions in §5.

## 2. DATA

To construct infrared luminosity functions, we use photometry from the Two Micron All Sky Survey (2MASS; Jarrett et al. 2000), and redshifts from the Las Campanas Redshift Survey (LCRS; Shectman et al. 1996). The LCRS consists of over 25,000 galaxies with redshifts, approximately covering the magnitude range  $R_c = 15$  to  $R_c = 17.7$ , where  $R_c$  is the “hybrid” Kron-Cousins  $R$  system described in Lin et al. (1996). The survey includes some fields observed with a 50 fiber configuration, and other, later fields observed with a 112 fiber configuration. The 50 fiber data are problematic because the sampling fraction is lower and the apparent magnitude range of the targeted galaxies is typically less than 1.5 magnitudes. Galaxies with high central surface brightnesses are excluded from the redshift survey, and this limit is about 0.7 mag fainter in the 50 fiber data. To ensure a homogeneous and maximally complete sample, we restrict ourselves to the 112 fiber data, as did Lin et al. (1996) for their fiducial computation of the optical LF.

We use the second incremental data release of the 2MASS catalog, which contains photometry in  $J$ ,  $H$  and  $K_s$  bands of both extended and point sources. The overlap of this release and the 112-fiber LCRS fields is patchy, covering only about 40% of the LCRS. Cross-correlation between the catalogs is done by matching galaxy astrometric positions. Following the example of Cole et al. (2000b), we allow matches between galaxies whose positions differ by less than 0.75 times the  $J$ -band Kron radius, to allow for the greater positional uncertainty of larger galaxies.

### 2.1. Spectral Classification

Zabludoff *et al.* (1996) measured the rest frame equivalent width of the  $[\text{OII}]\lambda 3727\text{\AA}$  emission line,  $W_o(\text{OII})$ , and the strength of the Balmer break,  $D_{4000}$ . We use  $W_o(\text{OII})$  to divide the sample into broad spectral classes: emission line (EL) galaxies with  $W_o(\text{OII}) \geq 5\text{\AA}$  and non-emission line (NEL) galaxies with  $W_o(\text{OII}) < 5\text{\AA}$ . Two caveats accompany this division. First, the  $[\text{OII}]$  line correlates with  $H\alpha$  emission, albeit with considerable scatter, suggesting that it is a good indicator of star formation in an average sense (e.g., Kennicutt 1992). However,  $W_o(\text{OII})$  also depends on metallicity and ionization, and on extinction if dust is non-uniformly distributed (i.e., more prevalent in HII regions; Charlot and Longhetti 2001). All of these properties are expected to depend on galaxy luminosity. The correlation between  $[\text{OII}]$  and  $H\alpha$  does indeed have a luminosity dependence (Tresse *et al.* 1999; Jansen *et al.* 2001). Second, although, the fibers used in the LCRS are quite large ( $3''.5$ ), Kochanek (2000a) suggests that aperture effects may still be important. We address this issue in §3.1.

### 2.2. Environment Classification

Group and cluster catalogs have been generated by Christlein (2000) from the LCRS using a friends-of-friends algorithm to search for overdensities in redshift space. For each association, the one dimensional velocity dispersion,  $\sigma_1$ , is computed. We define galaxy clusters to be those with  $\sigma_1 > 400\text{ km/s}$ , corresponding to a virial temperature of about 1 keV. Associations with smaller  $\sigma_1$  are termed “groups” and any galaxy not found to be in an overdense region is assigned to the “field” sample. Only associations with at least three members are retained in the final catalog; we discuss the possibility of biases related to this effect both below and in §2.4.

Velocity dispersions computed from small samples are biased low due to insufficient sampling of the wings of the distribution and the poor, biased determination of the mean (Zabludoff and Mulchaey 1998). This bias results in some fraction of the associations that properly belong in the “cluster” sample being incorrectly placed into the “group” sample. Furthermore, identification of groups with low velocity dispersions is sensitive to the linking length used in the cluster-finding algorithm, and such groups are more likely to be contaminated by interlopers. This contamination results in some groups that are false detections,

and the galaxies in those “groups” should be properly identified as isolated galaxies. To the degree that the environments are misclassified, any underlying differences among environments will be diluted.

### 2.3. Completeness

We compute the luminosity functions in both the  $K_s$  band, which is commonly used, and the  $J$  band, where the 2MASS photometry is deepest. In  $J$ , we use the Kron aperture magnitudes as the best estimate of the total magnitude. Cole *et al.* (2000b) demonstrate that the most robust  $K_s$  magnitudes are obtained by combining the Kron  $J$ -magnitudes with the default  $J - K_s$  colors. This nonintuitive result arises because the  $J$  images have a higher signal-to-noise ratio and allow a more accurate determination of the Kron aperture size. We adopt this magnitude definition of  $K_s$ . A small fraction (2.2%) of the galaxies in the LCRS within our magnitude range (defined below) are misclassified as stars in 2MASS. For these galaxies, we use the  $8''$  aperture magnitudes in the point source catalog.

It is important to check the overall completeness of the matched LCRS-2MASS catalog used in our analysis. In Figure 1 we show the fraction of the galaxies in 2MASS for which a successful match is made with a galaxy in the LCRS. We restrict our comparison to the largest ( $20^\circ \times 1.5^\circ$ ) contiguous patch covered by both surveys, which includes about 1300 galaxies. The LCRS is not intended to be complete, but is a random sample of a magnitude-limited survey. The dashed line shows the effect of applying the weights necessary to correct for this incompleteness. At  $K_s > 12.2$  and  $J > 13.2$ , the corrected completeness is close to 100%. At brighter magnitudes, the completeness drops, due primarily to the LCRS’s upper magnitude cutoff ( $R \sim 15$ ); we therefore limit the sample to magnitudes fainter than this limit. Cole *et al.* (2000b) show that 2MASS is highly complete and is not missing a substantial number of low surface brightness galaxies. By association there can be no significant incompleteness in low surface brightness galaxies in the matched LCRS-2MASS catalog, at least to the relatively bright lower magnitude limit of 2MASS.

The 2MASS catalog is complete to  $K_s = 13.2$ , and  $J = 14.5$ , as shown by Cole *et al.* (2000b). Up to about 0.5 mag fainter than these limits, the incompleteness is primarily due to misclassification of faint galaxies as stars and small biases in the magnitude measurements. We mitigate some of

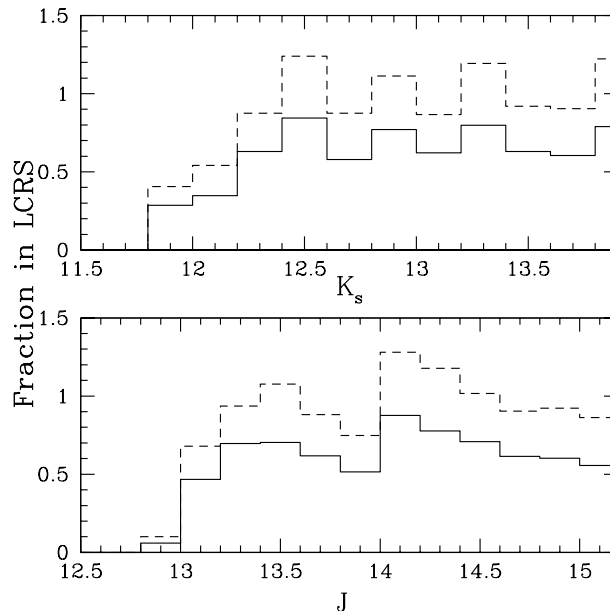


FIG. 1.— The completeness of the LCRS, relative to 2MASS, as a function of  $J$  and  $K_s$  magnitudes. The solid line shows the fraction of galaxies in the 2MASS catalog that have a corresponding match in the LCRS spectroscopic catalog. The dotted line shows the result of weighting the LCRS counts to account for the sampling fraction. The incompleteness at the bright end is due to the bright magnitude cutoff of the LCRS.

this incompleteness by using the LCRS to identify galaxies that 2MASS has classified as stars. Furthermore, because our sample is considerably smaller than that of Cole *et al.*, we are less concerned with systematic biases of order  $\lesssim 0.1$  mag, and we can maximize our useful sample size by considering fainter magnitude limits.

One other way to test the completeness of our sample is by considering the distribution of  $V/V_{\max}$ . For a galaxy at redshift  $z$ ,  $V(z)$  is the volume between it and the lowest redshift  $z_{\min}$  at which it would still have been selected in the sample (due to the bright magnitude limit).  $V_{\max}$  is the volume between  $z_{\min}$  and  $z_{\max}$ , where  $z_{\max}$  is the redshift at which the galaxy would drop out of the sample due to the faint magnitude limit. For a uniform spatial distribution of objects the mean value of  $V/V_{\max}$  is 0.5. Although galaxies are clustered, we expect that over the large volume surveyed here the distribution can be thought of as uniform. In Figure 2 we show the distribution of  $V/V_{\max}$  for the  $K_s$  band sample, limited at  $K_s = 13.7$ , and the  $J$  band sample, limited at  $J = 15.0$ . With these limits, the distribution of  $V/V_{\max}$  is approximately uniform, though there is a systematic variation of about 15%. The mean value of  $V/V_{\max}$  is about  $3\sigma$  larger than the value of 0.5, which it would be for a statistically complete sampling of a spatially uniform population. This appears to be partly due to a deficit

of galaxies with  $V/V_{\max} < 0.3$ , perhaps a consequence of Malmquist bias becoming important at  $K_s > 13.5$ . Indeed, moving the magnitude limit brighter by 0.2 mag does make the distribution of  $V/V_{\max}$  more uniform. None of the trends we discuss in this paper are affected by decreasing the magnitude limit, although the uncertainties are increased and, consequently, the significance of the results is diminished. To maximize the useful sample size, we therefore restrict the  $K_s$  sample to  $12.2 < K_s < 13.7$ , which consists of 2673 galaxies (including 274 cluster galaxies and 954 group galaxies). In  $J$ , we consider the sample of 3408 galaxies with  $13.2 < J < 15.0$  (including 346 cluster galaxies and 1202 group galaxies).

#### 2.4. Potential Biases and Systematic Uncertainties

Clusters and groups (associations) are defined by identifying friends-of-friends in redshift space. Only associations with three or more members are retained in the final catalog. A concern is that near this cutoff, associations with steeper faint end slopes  $\alpha$ , or brighter characteristic magnitudes, might be preferentially included in the catalog because more member galaxies would be above the magnitude limit. This could bias the final LF; however, we expect the overall effect to be small because the majority of the associations in our catalogue have more than the minimum three members, and are unlikely to drop below

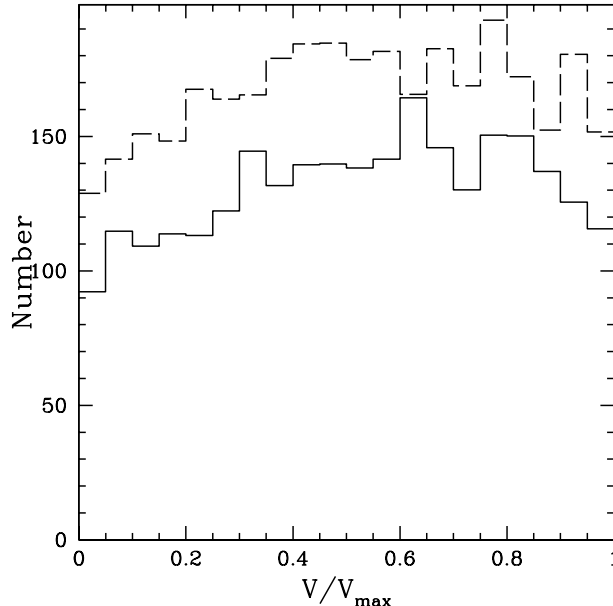


FIG. 2.— The distribution of  $V/V_{\max}$ , for the  $K_s$  band sample (*solid line*), limited at  $K_s = 13.7$ , and the  $J$  band sample (*dashed line*) limited at  $J = 15.0$ . The mean value is  $0.521 \pm 0.006$  for the  $K_s$  sample and  $0.513 \pm 0.005$  for the  $J$  sample.

this threshold given reasonable variations in the LF. To test for this potential effect, we have constructed mock catalogs, as described in Christlein (2000), by adding  $\sim 350,000$  artificial associations to the LCRS catalog. In one catalog, the associations have LFs with steep faint end slopes of  $\alpha = -1.2$ , and in another they have shallow slopes,  $\alpha = -0.6$ . As expected, we find no evidence from this experiment that the recovery fraction of associations with steeper faint-end slopes is higher than for those with flatter slopes. Thus, this potential bias does not have a significant effect on our selection, even when considering mock samples containing many more galaxies than the actual data.

There is a potential bias in any redshift catalog to be more complete in emission line galaxies because it is easier to measure redshifts for these galaxies than for non-emission line galaxies. This bias is particularly acute for the faintest galaxies in the sample. The magnitude ranges of the LCRS and 2MASS are not well matched, so only the brightest galaxies in the LCRS are included in our sample. In particular, most of the galaxies have  $15 < R_c < 16.5$ , well above the completeness limit of the LCRS. Because the magnitude range is small, and because we are far from the magnitude limit of the LCRS, there is little danger that a weak magnitude-dependent completeness function of the NEL galaxies has much effect on our analysis. In Figure 3 we show the  $V/V_{\max}$

distributions for the NEL and EL galaxies in the  $K_s$  selected sample. For the emission line galaxies,  $\langle V/V_{\max} \rangle = 0.515 \pm 0.008$ , while for the NEL galaxies  $\langle V/V_{\max} \rangle = 0.525 \pm 0.008$ . There is no evidence that the completeness of the EL sample differs from that of the NEL sample.

### 3. RESULTS

We compute the luminosity functions using both the non-parametric method of Efstathiou, Ellis & Peterson (1988, EEP) and by assuming a Schechter (1976) function shape as described by Sandage, Tamman & Yahil (1979, STY). Luminosities are calculated assuming an  $\Omega = 1$ ,  $\Lambda = 0$  cosmology, with the Hubble constant parametrized as  $H_0 = 100h \text{ km s}^{-1} \text{ Mpc}^{-1}$ . Where not explicitly shown, we use  $h = 1$ .  $K$ -corrections are taken from Poggianti (1997); they are small (less than 0.1 mag at  $z = 0.1$ ) and nearly independent of galaxy type. We neglect evolutionary corrections and extinction effects, both of which affect the magnitudes at less than the 0.1 mag level (e.g., Cole *et al.* 2000b).

We do not compute volume densities to normalize the luminosity functions. An estimate of the global normalization has already been presented in Cole *et al.* (2000b). For the field galaxies and the total sample, we normalize the luminosity functions to the weighted number of galaxies brighter than  $M_{K_s} = -21.5$  and  $M_J = -20.5$ . For the group and cluster environments, we divide by

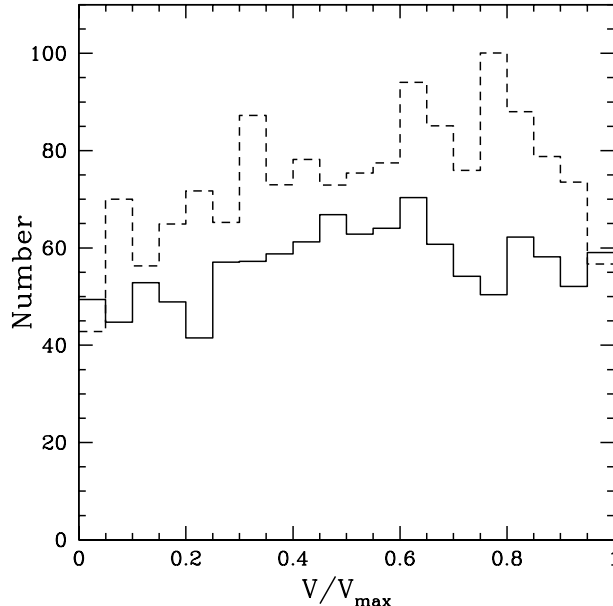


FIG. 3.— For the  $K_s$  selected sample, the distribution of  $V/V_{\max}$  for emission line galaxies (solid line) and NEL galaxies (dashed line). The mean value is  $0.515 \pm 0.008$  for the emission line galaxies and  $0.525 \pm 0.008$  for the NEL galaxies.

the number of associations to obtain the number of galaxies per group or cluster that are brighter than this limit.

In Figure 4 we show the  $J$  and  $K_s$ -band luminosity functions for the full sample. Both are well fit by Schechter functions with parameters  $M_{K_s}^* = -23.48 + 5\log h$ ,  $\alpha_{K_s} = -1.10$ , and  $M_J^* = -22.23 + 5\log h$ ,  $\alpha_J = -0.96$ . In the non-parametric method, the uncertainties are determined from the information matrix (EEP). The uncertainties in the Schechter parameters are determined from contours of the likelihood function, and are shown as 67% confidence elliptical contours in Figure 5. In Figure 5, we compare our result with recent measurements by Kochanek *et al.* (2000b) and Cole *et al.* (2000b). As shown in Cole *et al.*, the small difference between their result and that of Kochanek *et al.* is mostly due to the difference in the magnitude definition (we use that of Cole *et al.*). For the  $K_s$  sample, we are in good agreement with Cole *et al.* For the  $J$  sample, the  $1\sigma$  contours do not overlap, which may reflect the incompleteness introduced by including galaxies 0.5 magnitudes fainter than the nominal 2MASS completeness limit. We recover the Cole *et al.* result if we impose the same magnitude limits. While statistically significant, the difference in the  $J$  band results is small, and does not affect our conclusions based on subdividing the sample according to spectral type and environment.

### 3.1. Dependence on Spectral Type

In Figure 6 we present the LFs divided by spectral type. In  $J$  and  $K_s$  the NEL galaxies have a significantly flatter faint-end slope than the EL galaxies; this result is also evident from the error ellipses in Figure 5.

Kochanek (2000a) has recently suggested that the fixed angular size of the fibers used to obtain the spectra leads to a substantial aperture related bias. To address the significance of this effect we show the fraction of NEL galaxies as a function of redshift,  $f_{\text{NEL}}(z)$ , in four bins of absolute magnitude (Figure 7). There is a weak trend, in the expected sense that more distant galaxies are more likely to have spectra with emission lines because the fixed aperture includes more of the galaxy (we have already shown, in §2.4, that this is not due to a redshift dependent incompleteness in NEL galaxies). Although low luminosity galaxies tend to be physically smaller than high luminosity galaxies, they also lie at preferentially lower redshifts in a magnitude-limited sample. Thus, we expect the two effects to partially cancel out and reduce the size of this bias.

### 3.2. Environmental Dependence

As described in §2, we divide our sample into three environmental categories, corresponding to field, groups, and clusters. In Figure 8 we show the luminosity functions of these three classes of galaxies, compared with the best fit Schechter

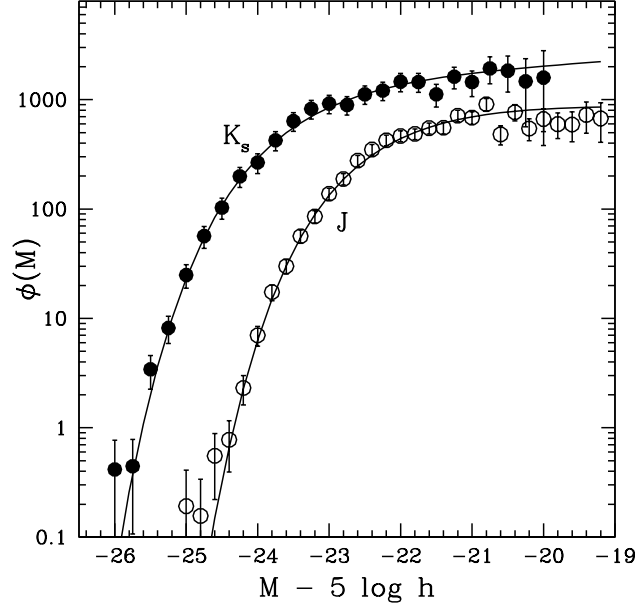


FIG. 4.— The  $J$  (*open symbols*) and  $K_s$ -band (*filled symbols*) luminosity functions. The points and solid lines are the determinations from the EEP and STY methods, respectively. The luminosity functions are arbitrarily normalized to the weighted number of galaxies brighter than  $M_{K_s} = -21.5$  and  $M_J = -20.5$  (the  $J$ -band LF is arbitrarily shifted vertically for clarity).

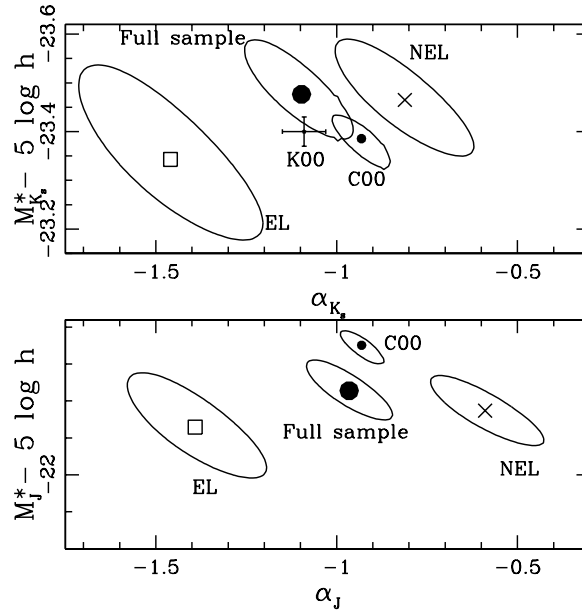


FIG. 5.— The error ellipses (67% confidence contours) on the Schechter parameters of the luminosity functions, for the full sample (*filled circle*), EL galaxies (*square*) and NEL galaxies (*cross*). Recent determinations by Kochanek et al. (2000) and Cole et al. (2000b) are marked K00 and C00 respectively. The small difference between the C00 and K00 results are due to the different magnitude systems used. All parameters are for  $\Omega = 1$ ,  $\Lambda = 0$ , and include only  $k$ -corrections, with no evolution.

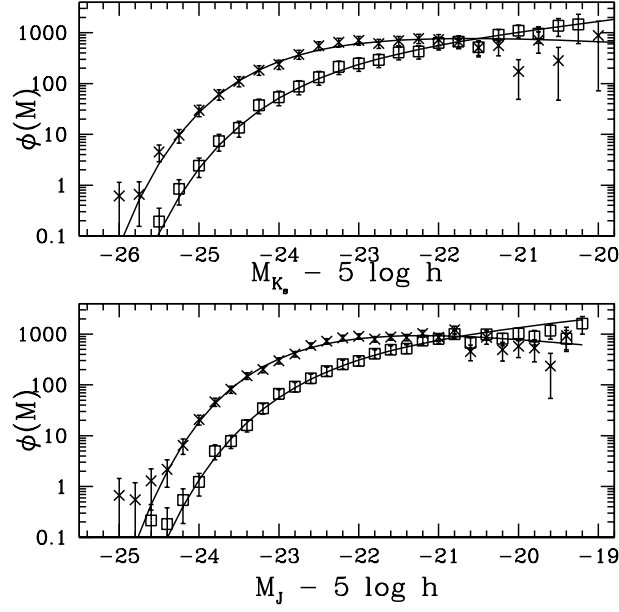


FIG. 6.— The  $J$  and  $K_s$ -band luminosity functions divided by spectral type. Open squares represent emission line galaxies, while crosses represent non-emission line galaxies. The luminosity functions are arbitrarily normalized to the weighted number of galaxies brighter than  $M_{K_s} = -21.5$  and  $M_J = -20.5$ .

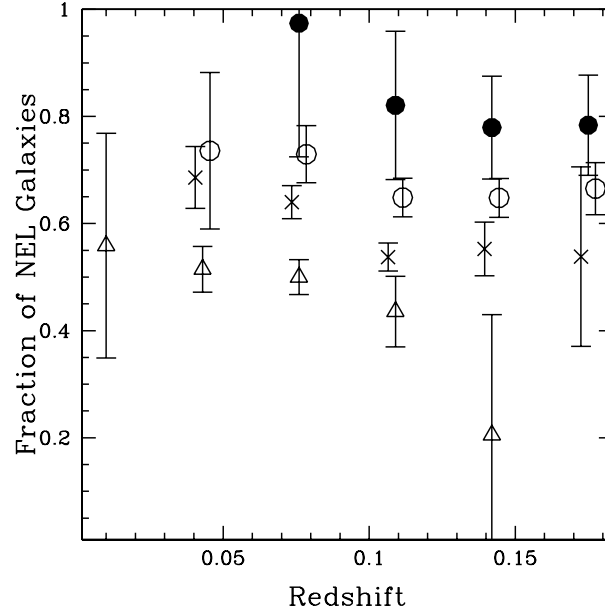


FIG. 7.— The fraction of NEL galaxies as a function of redshift is shown in the for four luminosity bins:  $-25.5 < M_{K_s} < -24.5$  (filled circles);  $-24.5 < M_{K_s} < -23.5$  (open circles);  $-23.5 < M_{K_s} < -22.5$  (crosses); and  $-22.5 < M_{K_s} < -21.5$  (triangles).



functions for the full sample; the 67% confidence error ellipses on the Schechter parameters are shown in Figures 9 and 10. The Schechter parameters of the  $J$ -band cluster LF are inconsistent with those of the field LF at the 95% confidence level, as determined from the likelihood contours. The trend is more significant in the  $J$ -band due to the larger sample size as a consequence of the deeper photometry. The difference is in the sense that the cluster LF has a brighter  $M_J^*$  and a steeper  $\alpha_J$ ; however, given the degeneracy between these parameters it is not clear precisely how the LF shape varies. If we restrict the Schechter fit to a limited luminosity range (e.g., brighter than  $M_J = -20.5$ , or fainter than  $M_J = -23.5$ ), the best-fit parameters change along the major axis of the error ellipse. However, both the cluster and field parameters move in the same direction, and the difference between them is approximately maintained. It appears, therefore, that the environmental dependence of the LF is not restricted to just the bright or faint end.

The differences among the LFs of different environments are larger when only the NEL galaxies are considered, as shown in Figure 9. In the field, the LF of NEL galaxies is much flatter than that of the full sample, but in clusters the LFs of EL and NEL are statistically indistinguishable. We discuss this result further in §4.3. The Schechter parameters of the  $J$  and  $K_s$  luminosity functions, for each data subsample, are tabulated in Table 1.

#### 4. DISCUSSION

##### 4.1. Comparison with Literature

It is encouraging that the global luminosity functions measured here, based on redshifts from the LCRS, are in such good agreement with recent determinations by Cole *et al.* (2000b) and Kochanek *et al.* (2000b). As shown by those authors, all infrared LFs derived from large samples are consistent (e.g., Mobasher *et al.* 1993; Glazebrook *et al.* 1995; Gardner *et al.* 1997; Szokoly *et al.* 1998; Loveday 2000). This concordance is in contrast with the historical situation at optical wavelengths, where there has been considerable disagreement between results in the literature. In particular, optical LFs derived from the LCRS (Lin *et al.* 1996; Christlein 2000) are generally shallower than most other measurements, and it has recently been shown that this difference results from an underestimation of galaxy magnitudes due to the shallow isophotal limit of

the LCRS photometry and from the exclusion of low central surface brightness galaxies (Blanton *et al.* 2000). The fact that we do not find a shallow slope in the infrared LF supports the interpretation that, at least over the relatively narrow, bright magnitude range of 2MASS, it is the  $R$  magnitudes, and not the survey selection itself, that is responsible for the discrepancy in the optical.

Analysis of the optical LF dependence on environment was done by Christlein (2000), using the LCRS sample. Although the LCRS magnitudes are systematically biased due to the bright isophotal limit, this bias applies uniformly to the whole sample and is therefore unlikely to affect the trends discussed in that paper. Christlein found strong evolution of the LF with environment, with the Schechter parameters changing along the major axis of the ellipse, toward steeper  $\alpha$  and brighter  $M^*$  with larger  $\sigma$ . The magnitude and sense of this change are fully consistent with the results presented in §3.2. The fact that Christlein finds such a continuous dependence on  $\sigma$  (something we are unable to investigate due to our smaller sample size) provides encouraging support that the effect is real. Zabludoff & Mulchaey (2000) found similar evidence for steep, bright  $R$ -band LFs in X-ray selected groups ( $\alpha = -1.3$ ). Because these groups generally have  $kT \gtrsim 1$  keV, many would be considered “clusters” by our criteria, and their results for steeper optical LFs in these systems are very similar to our results for the cluster infrared LFs.

Previously published evidence for an environmental dependence of the infrared LF is not as strong as for the optical LF. Both De Propris *et al.* (1998) and Andreon & Pelló (2000) find a steep faint end slope in the  $H$  band LF of the Coma cluster, but only at magnitudes fainter than our sample probes. Trentham & Mobasher (1998) find no evidence for a difference between the  $K$ -band LFs of cluster and field galaxies, over  $-24 < M_K < -22$ , although the uncertainties are large. Our sample is the first that is large enough to detect this weak effect at these luminosities. We look forward to dramatically improving the precision of this result when the full 2MASS catalog is released.

##### 4.2. The Stellar Mass Function

Do the observed dependencies of the infrared LF on environment and spectral type necessarily imply an analogous difference in the stellar mass functions? The infrared light is a good, but not

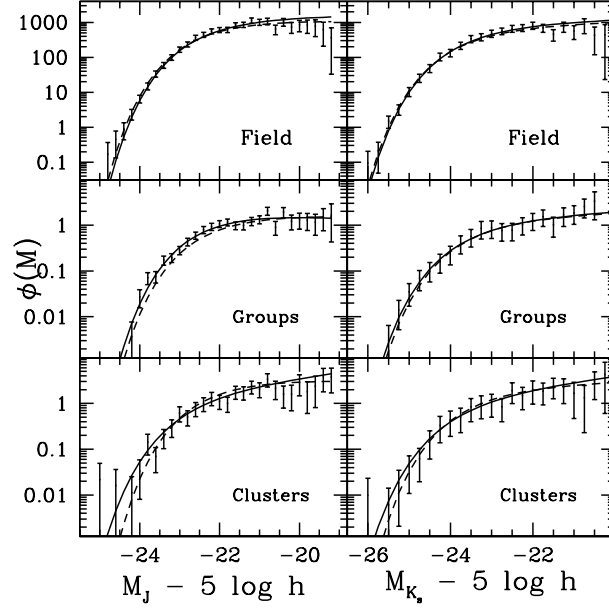


FIG. 8.— The  $J$  and  $K_s$ -band luminosity functions as a function of environment, shown as the error bars (EEP method) and the *solid lines* (STY method). The luminosity functions are arbitrarily normalized to the weighted number of galaxies brighter than  $M_{K_s} = -21.5$  and  $M_J = -20.5$ , divided by the number of groups or clusters as appropriate in the lower two panels. The *dashed lines* show the (arbitrarily renormalized) luminosity function for the whole sample for comparison. In most cases, this curve is hidden by the overlapping luminosity functions.

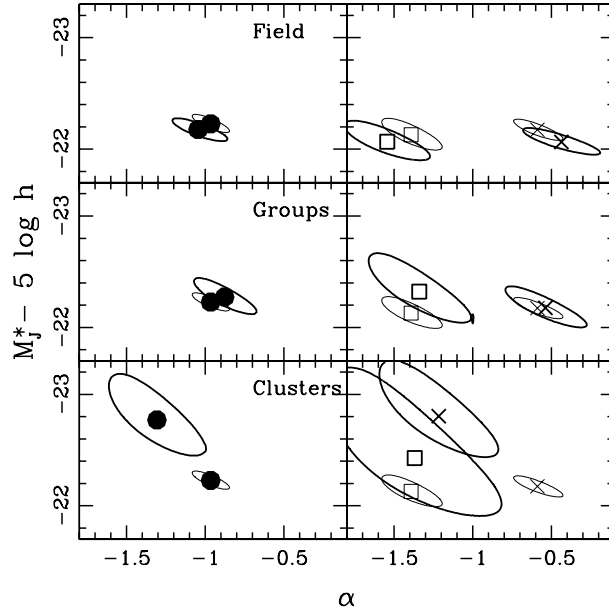


FIG. 9.— The 67% confidence error ellipses of the  $J$ -band Schechter fits for galaxies divided by environment. On the *left* are results for galaxies in the field (*top*), group (*middle*) and cluster (*bottom*) samples. The heavy ellipses correspond to the Schechter parameters for that bin; the lighter ellipses correspond to the Schechter parameters for the total sample, reproduced in each panel for comparison. On the *right* side of the figure, the samples are divided into EL and NEL galaxies. The best fit values for the emission line galaxies are indicated with a square, and the values for the NEL galaxies with a cross. All parameters are for  $\Omega = 1$ ,  $\Lambda = 0$ , and include only  $k$ -corrections, with no evolution.

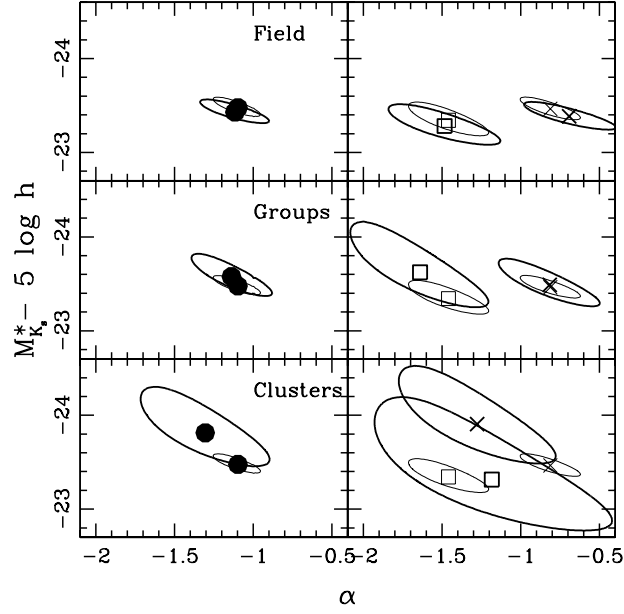


FIG. 10.— As Figure 9, for the  $K_s$  band data.

Environment	Spectral Type	$M_{K_s}^*$	$\alpha_{K_s}$	$M_J^*$	$\alpha_J$
Total	all	$-23.48 \pm 0.08$	$-1.10 \pm 0.14$	$-22.23 \pm 0.07$	$-0.96 \pm 0.12$
	EL	$-23.34 \pm 0.16$	$-1.46 \pm 0.26$	$-22.13 \pm 0.14$	$-1.39 \pm 0.19$
	NEL	$-23.46 \pm 0.12$	$-0.81 \pm 0.28$	$-22.17 \pm 0.09$	$-0.59 \pm 0.15$
Field	all	$-23.43 \pm 0.12$	$-1.12 \pm 0.21$	$-22.18 \pm 0.10$	$-1.04 \pm 0.18$
	EL	$-23.28 \pm 0.20$	$-1.48 \pm 0.36$	$-22.07 \pm 0.17$	$-1.54 \pm 0.27$
	NEL	$-23.38 \pm 0.16$	$-0.69 \pm 0.28$	$-22.06 \pm 0.10$	$-0.44 \pm 0.24$
Groups	all	$-23.58 \pm 0.13$	$-1.14 \pm 0.26$	$-22.37 \pm 0.17$	$-0.88 \pm 0.20$
	EL	$-23.62 \pm 0.44$	$-1.64 \pm 0.43$	$-22.32 \pm 0.29$	$-1.34 \pm 0.34$
	NEL	$-23.49 \pm 0.26$	$-0.81 \pm 0.33$	$-22.18 \pm 0.17$	$-0.54 \pm 0.27$
Clusters	all	$-23.81 \pm 0.40$	$-1.30 \pm 0.43$	$-22.77 \pm 0.34$	$-1.30 \pm 0.32$
	EL	$-23.31 \pm 0.70$	$-1.18 \pm 0.76$	$-22.43 \pm 0.65$	$-1.37 \pm 0.56$
	NEL	$-23.91 \pm 0.52$	$-1.28 \pm 0.50$	$-22.80 \pm 0.43$	$-1.22 \pm 0.39$

TABLE 1

WE USE THE COSMOLOGICAL PARAMETERS  $\Omega = 1$ ,  $\Lambda = 0$ ,  $h = 1$ . THE TABULATED  $1\sigma$  ERRORS ARE STRONGLY CORRELATED, AS SHOWN BY THE ERROR ELLIPSES IN FIGURES 5, 9 AND 10.

perfect tracer of the stellar mass; the mass-to-light ratio ( $M/L$ ) can be expected to increase by about a factor of two between early- and late-type galaxies (e.g., Bell and de Jong 2001). To estimate  $M/L$ , constraints on the mean stellar age are required. The optical-IR colors of our sample are unreliable due to the shallow isophotal limit of the LCRS, and the IR colors alone are insensitive to stellar population differences. The best indicator available to us is therefore the  $D_{4000}$  spectral index from the LCRS spectra. We use the solar-metallicity models of Fiac & Rocca-Volmerange (1997) to generate spectra from a given star formation history. We then compute  $D_{4000}$  directly from the spectra, using the same definition as Zabludoff *et al.* (1996). The correlation between  $M/L_J$  and  $D_{4000}$  depends only weakly on star formation history. Figure 11 shows model results for a single burst, simple stellar population (SSP) and for a galaxy with a constant star formation rate, using a Kennicutt (1983) initial mass function. The two models can differ by as much as 40%, over a narrow range of  $D_{4000}$ , but the ranking with  $M/L$  is unchanged.  $D_{4000}$  is sensitive to metallicity and reddening, which we neglect, but is less sensitive than optical colors. For example, an extinction of  $A_V = 1.5$  magnitudes only reddens  $D_{4000}$  by about 0.2.

In Figure 12 we show the 67% and 95% error ellipses on the Schechter parameters for the stellar mass functions derived using the  $M/L$  corrections derived from the SSP model. The differences observed in the luminosity functions are *exacerbated* in the stellar mass functions. Thus, we conclude that the stellar mass function is not universal, but depends on both galaxy type and the local environment.

#### 4.3. Implications and Speculations

Both Christlein (2000) and Zabludoff & Mulchaey (2000) find that the change in the optical LF shape with environment is due almost exclusively to the NEL galaxies. We confirm that the difference in the infrared cluster LF, relative to the field, is dominated by this population. It is interesting that the faint end slope of the NEL galaxies in clusters, as parametrized by  $\alpha$ , is similar to that of the overall field faint end slope. One interpretation for this similarity is that the bulk of the cluster population is built up by accreting field galaxies with little effect other than the cessation of star formation, as modeled for example by Balogh, Navarro & Morris (2000). However, from only the agreement of the LFs, we cannot

exclude scenarios in which the similar initial progenitors of faint galaxies in various environments began forming stars at different times (the cluster ones earlier by virtue of originating near a large mass perturbation). In the latter scenario, one expects the field LF to evolve to the cluster LF in time, as gas is consumed by galaxies and their star formation stops.

In Figure 13 we show the fraction of NEL galaxies as a function of luminosity for the global sample. This Figure shows a strong trend that, unfortunately, is difficult to interpret because metallicity and extinction also correlate with luminosity in a way that makes [OII] stronger in low luminosity galaxies (e.g., Jansen 2001). We cannot infer the extent to which this relation indicates an inherent correlation between galaxy mass and instantaneous star formation rate — a correlation that would be an important test of galaxy formation models. In particular, a variation in the fraction of currently star forming galaxies with mass could indicate that the dominant mode of star formation (i.e., burst-like or continuous) for a galaxy in the field is mass dependent (e.g., Kauffmann, Charlot & Balogh, in preparation).

## 5. CONCLUSIONS

We have measured the  $J$  and  $K_s$ -band galaxy luminosity functions from the 2MASS, using redshifts from the LCRS, and divided the sample based on spectral type and environment. We draw the following conclusions:

- In non-cluster environments, the infrared luminosity function of emission line (EL) galaxies is steeper than that of non-emission line (NEL) galaxies.
- There is a statistically significant difference between the cluster and field galaxy infrared luminosity functions, in the sense that  $M^*$  is brighter, and the faint end slope  $\alpha$  is steeper, in clusters.
- Using the  $D_{4000}$  spectral index from the LCRS spectra to aid us in converting from infrared luminosity to stellar mass, we conclude that the results just described also hold for the stellar mass functions and, in fact, the differences are more pronounced.
- The shape of the NEL galaxy stellar mass function in clusters is similar to that of the global stellar mass function in the field. One explanation of this trend is that the cluster is mostly built up of field EL galaxies, in which

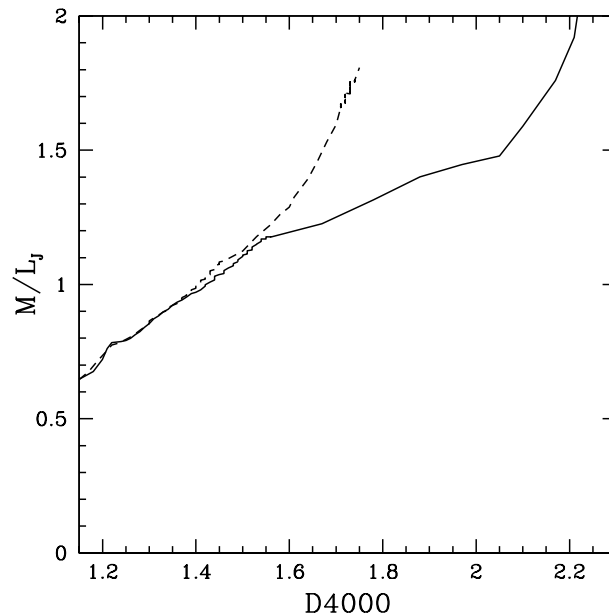


FIG. 11.— Mass-to-light ratio in the  $J$  band, as a function of  $D_{4000}$ , for a Kennicutt (1983) initial mass function from the models of Fioc & Rocca-Volmerange (1997). The solid line is a single burst population, and the dashed line represents a galaxy with constant star formation rate. In both models, the galaxy evolves from left to right with time, reaching its maximum  $D_{4000}$  at 13 Gyr.

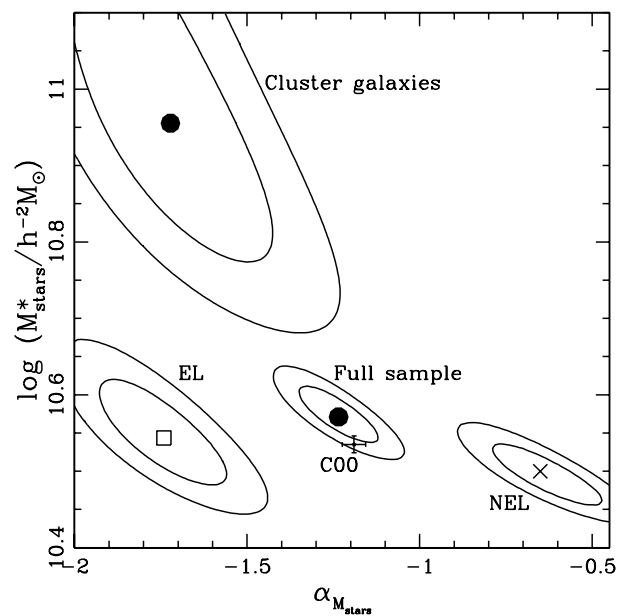


FIG. 12.— 67% and 95% confidence ellipses on the Schechter parameters for various stellar mass functions, using  $J$ -band mass-to-light ratios determined from the  $D_{4000}$  index, as described in the text. The point with error bars is the result of Cole *et al.* (2000b) using the Kennicutt (1983) initial mass function. The differences in luminosity function shape when divided by spectral type and environment are even more pronounced in the stellar mass functions than in the luminosity functions.

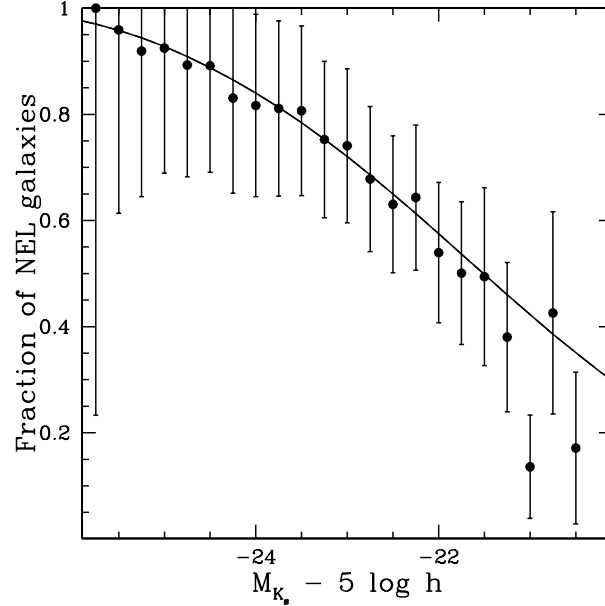


FIG. 13.— The fraction of non-emission line galaxies as a function of luminosity, as determined by the non-parametric luminosity function (points) and the Schechter function fits (solid line).

star formation has ceased either because (1) the galaxies consumed all their gas (either through accelerated star formation due to the cluster environment, or by forming earlier due to their proximity to a large mass perturbation); or (2) they lost some or all their gas through processes like ram pressure stripping.

#### ACKNOWLEDGEMENTS

We thank Guinevere Kauffmann for suggesting the idea of comparing the 2MASS and LCRS catalogs. We are also grateful to the LCRS collaboration for making the spectra available. MLB acknowledges support from a PPARC rolling grant for extragalactic astronomy and cosmology at Durham. DC and AIZ acknowledge financial support from NASA grant GO0-1007X. DZ acknowledges financial support from a NSF CAREER grant (AST-9733111), and a fellowship from the David and Lucile Packard Foundation.

#### REFERENCES

- Andreon, S. and Pelló, R.: 2000, *A&A* **353**, 479  
 Balogh, M. L., Morris, S. L., Yee, H. K. C., Carlberg, R. G., and Ellingson, E.: 1997, *ApJL* **488**, 75  
 Balogh, M. L., Navarro, J. F., and Morris, S. L.: 2000, *ApJ* **540**, 113  
 Balogh, M. L., Pearce, F. R., Bower, R. G., and Kay, S. T.: 2001, *MNRAS* submitted  
 Balogh, M. L., Schade, D., Morris, S. L., Yee, H. K. C., Carlberg, R. G., and Ellingson, E.: 1998, *ApJL* **504**, 75  
 Bardeen, J. M., Bond, J. R., Kaiser, N., and Szalay, A. S.: 1986, *ApJ* **304**, 15  
 Bell, E. F. and de Jong, R. S.: 2001, *ApJ* **550**, 212  
 Binggeli, B., Sandage, A., and Tammann, G. A.: 1988, *ARA&A* **26**, 509  
 Blanton, M. and the SLOAN collaboration: 2000, *astro-ph/0012085*  
 Bromley, B. C., Press, W. H., Lin, H., and Kirshner, R. P.: 1998, *ApJ* **505**, 25  
 Charlot, S. and Longhetti, M.: 2001, *astro-ph/0101097*  
 Christlein, D.: 2000, *ApJ* in press  
 Cole, S.: 1991, *ApJ* **367**, 45  
 Cole, S., Lacey, C. G., Baugh, C. M., and Frenk, C. S.: 2000a, *MNRAS* **319**, 168  
 Cole, S., Norberg, I. R. P., Baugh, C. M., Frenk, C. S., and the 2dFGRS team: 2000b, *astro-ph/0012429*  
 de Propris, R., Eisenhardt, P. R., Stanford, S. A., and Dickinson, M.: 1998, *ApJL* **503**, L45  
 de Propris, R., Pritchet, C. J., Harris, W. E., and McClure, R. D.: 1995, *ApJ* **450**, 534+  
 Dressler, A., Thompson, I. B., and Shectman, S. A.: 1985, *ApJ* **288**, 481  
 Efstathiou, G., Ellis, R. S., and Peterson, B. A.: 1988, *MNRAS* **232**, 431  
 Ellis, R. S., Colless, M., Broadhurst, T., Heyl, J., and Glazebrook, K.: 1996, *MNRAS* **280**, 235  
 Ferguson, H. C. and Sandage, A.: 1991, *AJ* **101**, 765  
 Fioc, M. and Rocca-Volmerange, B.: 1997, *A&A* **326**, 950  
 Folkes, S., Ronen, S., Price, I., Lahav, O., Colless, M., Maddox, S., Deeley, K., Glazebrook, K., Bland-Hawthorn, J., Cannon, R., Cole, S., Collins, C., Couch, W., Driver, S. P., Dalton, G., Efstathiou, G., Ellis, R. S., Frenk, C. S., Kaiser, N., Lewis, I., Lumsden, S., Peacock, J., Peterson, B. A., Sutherland, W., and Taylor, K.: 1999, *MNRAS* **308**, 459  
 Gardner, J. P., Sharples, R. M., Frenk, C. S., and Carrasco, B. E.: 1997, *ApJL* **480**, 99  
 Gavazzi, G., Pierini, D., and Boselli, A.: 1996, *A&A* **312**, 397  
 Glazebrook, K., Peacock, J. A., Miller, L., and Collins, C. A.: 1995, *MNRAS* **275**, 169  
 Granato, G. L., Lacey, C. G., Silva, L., Bressan, A., Baugh, C. M., Cole, S., and Frenk, C. S.: 2000, *ApJ* **542**, 710  
 Jansen, R. A., Franx, M., and Fabricant, D.: 2001, *astro-ph/0012485*  
 Jarrett, T. H., Chester, T., Cutri, R., Schneider, S., Skrutskie, M., and Huchra, J. P.: 2000, *AJ* **119**, 2498  
 Kennicutt, R. C.: 1983, *ApJ* **272**, 54  
 Kennicutt, R. C.: 1992, *ApJ* **388**, 310  
 Kocharnek, C. S., Pahre, M. A., and Falco, E. E.: 2000a, *astro-ph/0011458*

- Kochanek, C. S., Pahre, M. A., Falco, E. E., Huchra, J. P., Mader, J., Jarrett, T. H., Chester, T., Cutri, R., and Schneider, S. E.: 2000b, *astro-ph/0011456*
- Lacey, C. and Cole, S.: 1993, *MNRAS* **262**, 627
- Larson, R. B.: 1974, *MNRAS* **169**, 229
- Lin, H., Kirshner, R. P., Shectman, S. A., Landy, S. D., Oemler, A., Tucker, D. L., and Schechter, P. L.: 1996, *ApJ* **464**, 60
- Loveday, J.: 2000, *MNRAS* **312**, 557
- Loveday, J., Peterson, B. A., Efstathiou, G., and Maddox, S. J.: 1992, *ApJ* **390**, 338
- Loveday, J., Tresse, L., and Maddox, S.: 1999, *MNRAS* **310**, 281
- Marzke, R. O. and da Costa, L. N.: 1997, *AJ* **113**, 185+
- Marzke, R. O., da Costa, L. N., Pellegrini, P. S., Willmer, C. N. A., and Geller, M. J.: 1998, *ApJ* **503**, 617+
- Marzke, R. O., Geller, M. J., Huchra, J. P., and Corwin, H. G.: 1994a, *AJ* **108**, 437
- Marzke, R. O., Huchra, J. P., and Geller, M. J.: 1994b, *ApJ* **428**, 43
- Mobasher, B., Sharples, R. M., and Ellis, R. S.: 1993, *MNRAS* **263**, 560
- Moore, B., Lake, G., Quinn, T., and Stadel, J.: 1999, *MNRAS* **304**, 465
- Moss, C. and Whittle, M.: 2000, *MNRAS* in press
- Narayanan, V. K., Berlind, A. A., and Weinberg, D. H.: 2000, *ApJ* **528**, 1
- Poggianti, B. M.: 1997, *A&ASS* **122**, 399
- Poggianti, B. M., Smail, I., Dressler, A., Couch, W. J., Barger, A. J., Butcher, H., Ellis, R. S., and Oemler, A.: 1999, *ApJ* **518**, 576
- Ratcliffe, A., Shanks, T., Parker, Q. A., and Fong, R.: 1998, *MNRAS* **293**, 197+
- Rees, M. J. and Ostriker, J. P.: 1977, *MNRAS* **179**, 541
- Sandage, A., Binggeli, B., and Tammann, G. A.: 1985, *AJ* **90**, 1759+
- Sandage, A., Tammann, G. A., and Yahil, A.: 1979, *ApJ* **232**, 352
- Schechter, P.: 1976, *ApJ* **203**, 297
- Shectman, S. A., Landy, S. D., Oemler, A., Tucker, D. L., Lin, H., Kirshner, R. P., and Schechter, P. L.: 1996, *ApJ* **470**, 172+
- Silva, L., Granato, G. L., Bressan, A., and Danese, L.: 1998, *ApJ* **509**, 103
- Szokoly, G. P., Subbarao, M. U., Connolly, A. J., and Mobasher, B.: 1998, *ApJ* **492**, 452
- Trentham, N. and Mobasher, B.: 1998, *MNRAS* **299**, 488
- Tresse, L., Maddox, S., Loveday, J., and Singleton, C.: 1999, *MNRAS* **310**, 262
- Treyer, M. A., Ellis, R. S., Milliard, B., Donas, J., and Bridges, T. J.: 1998, *MNRAS* **300**, 303
- White, S. D. M., Davis, M., Efstathiou, G., and Frenk, C. S.: 1987, *Nature* **330**, 451
- Zabludoff, A. I. and Mulchaey, J. S.: 1998, *ApJ* **496**, 39+
- Zabludoff, A. I. and Mulchaey, J. S.: 2000, *ApJ* **539**, 136
- Zabludoff, A. I., Zaritsky, D., Lin, H., Tucker, D., Hashimoto, Y., Shectman, S. A., Oemler, A., and Kirshner, R. P.: 1996, *ApJ* **466**, 104
- Zucca, E., Zamorani, G., Vettolani, G., Cappi, A., Merighi, R., Mignoli, M., Stirpe, G. M., MacGillivray, H., Collins, C., Balkowski, C., Cayatte, V., Maurogordato, S., Proust, D., Chincarini, G., Guzzo, L., Maccagni, D., Scaramella, R., Blanchard, A., and Ramella, M.: 1997, *A&A* **326**, 477